B-PHYSICS WITH EXISTING COLLIDER DETECTORS

Anne Kernan
University of California, Riverside

ABSTRACT

B-hadrons are copiously produced at the CERN and Fermilab proton-antiproton colliders. B-physics results from the UA1 experiment at CERN are summarised here, and prospects for future studies with the UA1, UA2, CDF and DØ collider detectors are examined. Particular attention is given to muon triggering capability.

1. INTRODUCTION

The measured cross section for $b\bar{b}$ production at the CERN proton-antiproton collider is around 1 μb, in agreement with QCD predictions [1]. At the Tevatron collider this cross section is expected to lie in the range 14 – 30 μb [2]; the corresponding production rate for luminosity 10^{30} $cm^{-2}s^{-1}$ exceeds 10^6 per day. To what extent can the "existing" collider detectors at CERN (UA1 and UA2) and Fermilab (CDF and DØ) exploit these large beauty production rates to investigate the rich phenomenology of the $B\bar{B}$ sector?

2. B-PHYSICS AT THE CERN COLLIDER

At the CERN collider b-quark studies in the UA1 experiment have relied on the observation of muons from the semi-leptonic decay of B-hadrons. At $\sqrt{s}$ of 630 GeV QCD expectations, as calculated in ISAJET [3], are that c/b-quark production is the dominant source of prompt muons with p_T below 20 GeV/c [1,4]. Beauty is expected to dominate over charm because of the harder fragmentation function of the b-quark.

Muons rather than electrons are used to tag heavy quark production in UA1 for two reasons:

1. Muons can be triggered down to p_T of 3 GeV/c in the UA1 detector whereas electrons are swamped by hadronic background at $p_T \lesssim 15$ GeV/c,
2. Leptons from C/B decay are part of a hadronic jet. Muons, but not electrons, are identifiable inside a jet.

The UA2 detector lacks a muon detection system. Consequently the UA2 collaboration has no plan for B-physics studies at the $Sp\bar{p}S$ [5].

2.1 Results from Experiment UA1

Current results come primarily from the 1984 and 1985 collider runs in which four million single muon and dimuon triggers were recorded for an integrated luminosity of 570 nb^{-1} at $\sqrt{s}$ of 630 GeV. Figure 1 shows the measured inclusive muon cross section for $p_T(\mu) > 6$ GeV/c where the transverse momentum is measured with respect to the incident beam direction [4]. Also shown is the estimated background from π/K decay in flight. Decay-in-flight background effectively overwhelms the prompt muon signal below p_T of 6 GeV/c.

Figure 2 shows the inclusive single muon spectrum after background subtraction [4]. The broken line is the distribution predicted by the ISAJET Monte Carlo program in combination with an exact simulation of the UA1 detector response and reconstruction programs. ISAJET indicates that prompt muons of $p_T < 20$ GeV/c come mainly from semi-leptonic decay of C- and B-hadrons. Table 1 from reference 4 gives a breakdown of the predicted contributions to the prompt inclusive muon cross section for the range $10 < p_T(\mu) < 15$ GeV/c. Beauty dominates over charm because of the harder fragmentation function of the b-quark. Given the uncertainty in integrated luminosity (±15%) and in the magnitude of the background subtraction, the agreement between the data and Monte Carlo is quite impressive.

Table 1. ISAJET cross-sections for processes contributing to the UA1 inclusive prompt muon spectrum in the range $10 < p_T^{\mu} < 15$ GeV/c, $|\eta^{\mu}| < 1.5$ [4]. The errors quoted for the Monte Carlo contributions are purely statistical.

PROCESS	CROSS-SECTION (nb)
Beauty, $b \rightarrow \mu$	2.45±0.03
Charm, $c \rightarrow \mu$	0.83±0.02
Drell-Yan, $J/\Psi, \Upsilon$	0.19±0.009
$W,Z \rightarrow \mu$	0.07±0.005
Total Monte Carlo	3.54±0.04
Data	$4.33 \pm 0.20^{+0.83}_{-0.56}$

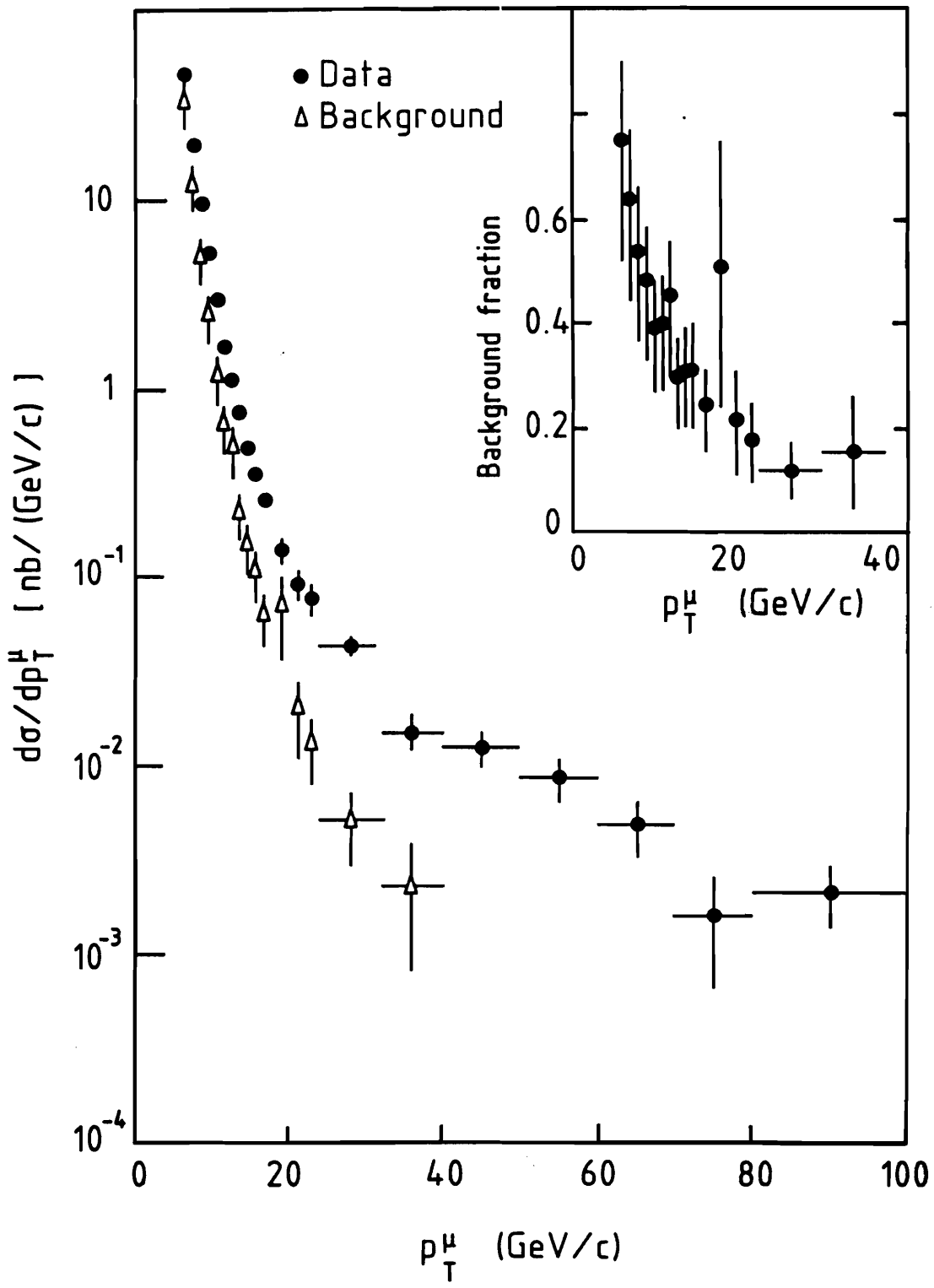

Fig. 1. Inclusive muon distribution (circles) and estimated decay-in-flight background (triangles) in the UA1 Experiment at $\sqrt{s}$ of 630 GeV [4]. The insert shows the background fraction as a function of p_T.

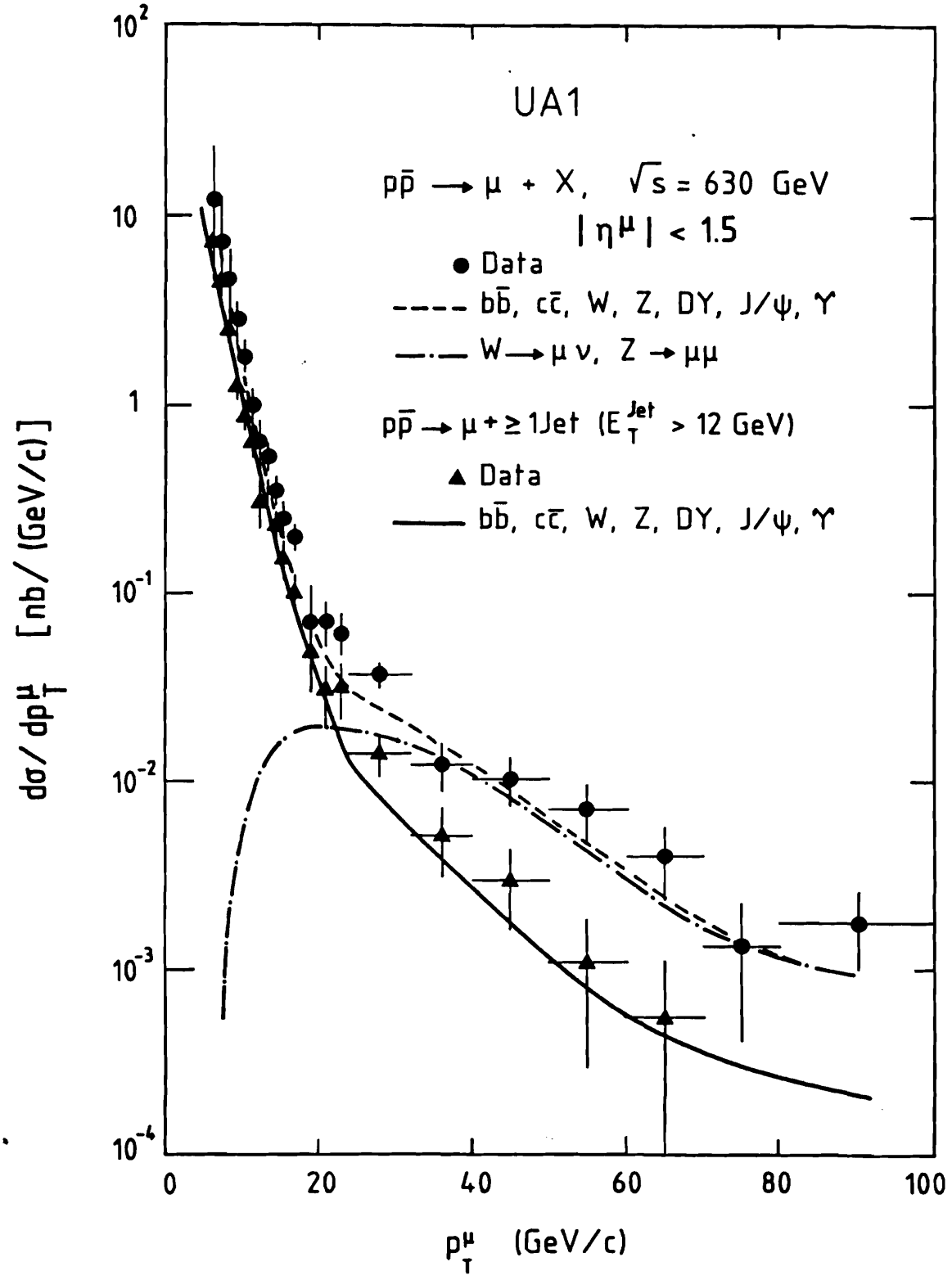

Fig. 2. Inclusive muon p_T spectrum (corrected for decay background and acceptance) for all events and for events with at least one jet with $E_T > 12$ GeV [4]. The curves show the ISAJET predictions for W, Z alone and for all for the processes listed in Table 1.

More direct evidence for the domination of beauty over charm is given in fig. 3 which shows the projection of the muon momentum transverse to the jet (charged particle) axis [4]. This distribution is fit with the ratio $c/(c + b) = 24 \pm 8 \pm 9$ %.

As described in reference 4, the ISAJET Monte Carlo program provides an exact calculation of $Q\bar{Q}$ ($Q \equiv c/b$) production cross sections in lowest order (flavor creation), and approximates the α_s^3 processes by "flavor excitation" and "gluon splitting" reactions in which an initial and final state gluon respectively evolve to $Q\bar{Q}$. Certain experimental distributions are sensitive to the relative amounts of the different production processes. Thus the angular separation of muon pairs in the transverse plane (fig. 4) is strongly peaked at 180° for creation while it is peaked near zero for gluon splitting [4]. Table 2 lists the relative amounts of the three processes predicted by ISAJET and inferred from a fit to the data in fig. 4. The data is consistent with the ISAJET prediction that each process accounts for approximately one third of the events. With increased statistics on dimuon events it should be possible to make detailed studies of $Q\bar{Q}$ production mechanisms in the future (Section 3.1.1)

Figure 5a compares the predicted parton-parton invariant mass distribution for strongly produced $Q\bar{Q}$ pairs with that for $W \rightarrow c\bar{s}$ and $Z \rightarrow c\bar{c}$, $b\bar{b}$. [6]. The $W/Z \rightarrow c/b$ decay channels, which exclude the copious background of QCD produced light quark and gluon jet pairs, have been searched for in the UA1 experiment. The W/Z signal in fig. 5a is seen to be comparable in magnitude to α_s^2 production of $Q\bar{Q}$, at the same $M(Q\bar{Q})$, but is however overwhelmed by the α_s^3 processes. Fig. 5b shows the experimental invariant mass distribution $M(\text{jet-jet-}\mu\text{-}\nu_T)$ in UA1 for jet pairs in which the presence of a muon with $p_T > 8$ GeV/c signals a c/b quark, and the missing transverse energy is ascribed to a neutrino. The predicted $W/Z \rightarrow c/b$ contribution to $M(\text{jet-jet-}\mu\text{-}\nu_T)$, also shown in fig 5b, is obviously undetectable. At the Tevatron the probability of observing W/Z decay to jets is even lower since the W/Z production cross section is expected to increase by a factor of three compared to a factor of nine increase in the strong $Q\bar{Q}$ cross section in the same $M(Q\bar{Q})$ mass range [6].

Table 2. ISAJET predictions and fitted values for the relative contributions of different QCD production processes to the dimuon events plotted in fig. 4.

QCD PROCESSES	ISAJET PREDICTION (%)	MEASURED (%)
Flavor Creation	33	45^{+16}_{-13}
Flavor Excitation	39	33^{+16}_{-13}
Gluon Splitting	28	22^{+20}_{-17}

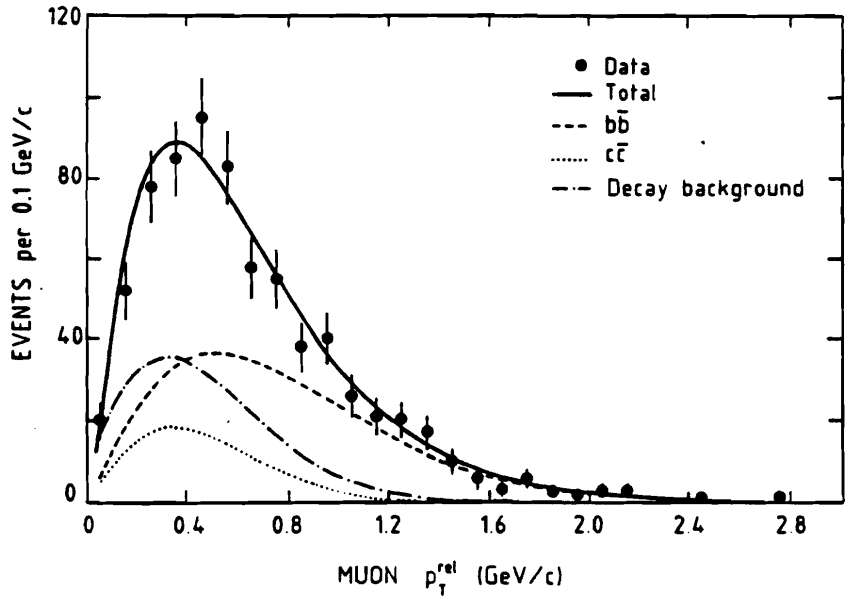

Fig. 3. Distribution in p_T^{rel}, the muon momentum transverse to the jet axis (defined as the summed charged particle momenta) for events having a muon with $p_T > 10$ GeV/c and at least one jet with $E_T > 10$ GeV/c [4]. The data was fitted with a variable ratio of $c\bar{c}$ to $b\bar{b}$ production and a decay-in-flight component fixed at 33% of the total.

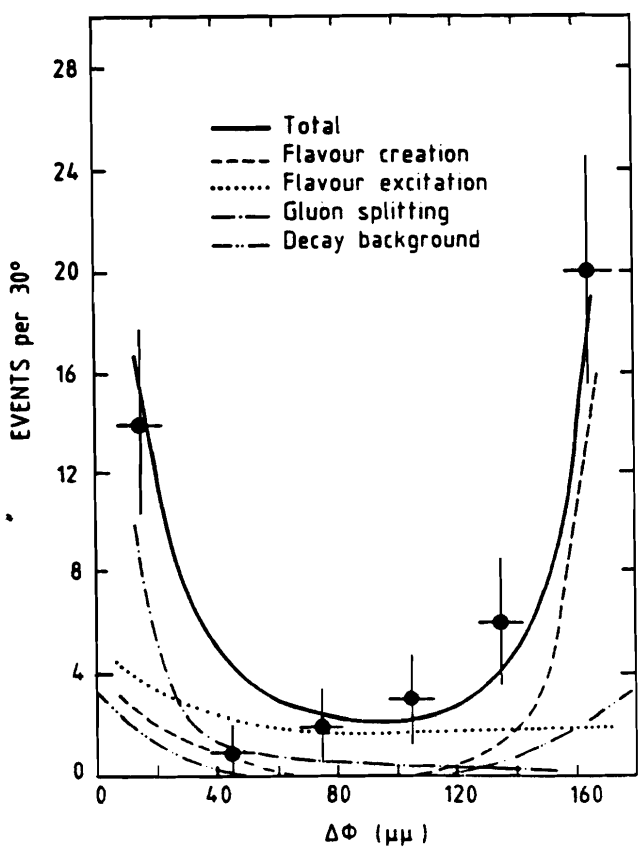

Fig. 4. Distribution in $\Delta\phi$, the angular separation of muon pairs in the transverse plane for events containing at least one "non-isolated" muon and a jet with $E_T > 12$ GeV [4]. The curves show a fit to the data with a fixed decay-in-flight background and varying amounts of the QCD production processes listed above.

A clear J/Ψ signal (fig. 6) is observed in dimuon events having $p_T(\mu) > 3$ GeV/c and $p_T(2\mu) > 4$ GeV/c: the sample consists of 434 dimuon events and 60 like sign muon pairs [7]. At $\sqrt{s}$ of 630 GeV the dominant production modes for high p_T J/Ψ are expected to be:

$$g + g \rightarrow \chi + g, \chi \rightarrow J/\Psi + \gamma , \quad \text{--- (1)}$$

$$B \rightarrow J/\Psi + X. \quad \text{--- (2)}$$

Figure 7 compares the measured p_T distribution for J/Ψ with that expected for χ and for B decay; the data suggests that production via χ decay dominates. The best estimate of component (2) is based upon the idea that a J/Ψ from B decay is accompanied by the fragments of the b-quark hadronization. Thus from fig. 8, which shows the distribution in ΔR^2, $(\Delta\phi^2 + \Delta\eta^2)$, of charged tracks with $p_T > 1$ GeV/c relative to the J/Ψ direction, it is inferred that the fraction of J/Ψ from B decay is $0.24 \pm 0.08 \pm 0.12$. The corresponding cross section for J/Ψ production via beauty decay, $\sigma \cdot B = 1.8 \pm 0.6 \pm 0.9$ nb, is consistent with the beauty cross section previously inferred from the dimuon signal in experiment UA1 [1].

A clear signal for upsilon decaying to muons was reported earlier in reference 1 (fig. 9).

2.2 Future B-Physics with the UA1 Detector.

The upgrade of the CERN proton-antiproton collider (ACOL project) is expected to provide a luminosity of 10^{30} $cm^{-2}s^{-1}$ for 1988 running and double that in subsequent years. The integrated luminosity for a four month run at maximum instantaneous luminosity of 2×10^{30} $cm^{-2}s^{-1}$ would then be about 5 pb^{-1}.

In the post-ACOL era additional shielding will be needed to preserve the UA1 triggering capability for inclusive muons [8]. Figure 10 shows the acceptance in pseudorapidity of the UA1 muon detector and the triggering limit for single muons in the 1985 run with $L_{max} = 4 \times 10^{29}$ and $\langle L_{fill} \rangle = 1.3 \times 10^{29}$; the dimuon trigger used the full detector. It will be necessary to insert 4.5 absorption lengths of iron in front of the forward elements of the muon detector to reduce decay-in-flight background in future runs. As shown in Table 3 this iron, as well as the increased thickness of the new U/TMP calorimeter, will reduce the single muon trigger rate to an acceptable level. The upgraded UA1 trigger and readout system will be able to accept a rate up to 25 Hz from the first level muon trigger.

The muon p_T thresholds for physics analysis are expected to remain unchanged at 6 GeV/c for single muons and 3 GeV/c for dimuons.

UA1 has reported evidence for $B^o - \bar{B}^o$ mixing from a study of 512 dimuon events with $M_{\mu\mu} > 6$ GeV/c^2 and $p_T > 3$ GeV/c for each muon [1]. In the next few years an integrated luminosity of 15 nb^{-1} could yield a sample of 10^4 dimuon events. Figure 11 shows the current UA1 mixing result with the one-standard-deviation bands scaled down to simulate a factor of twenty increase in statistics [8]. The increased precision in the measurement of the mixing

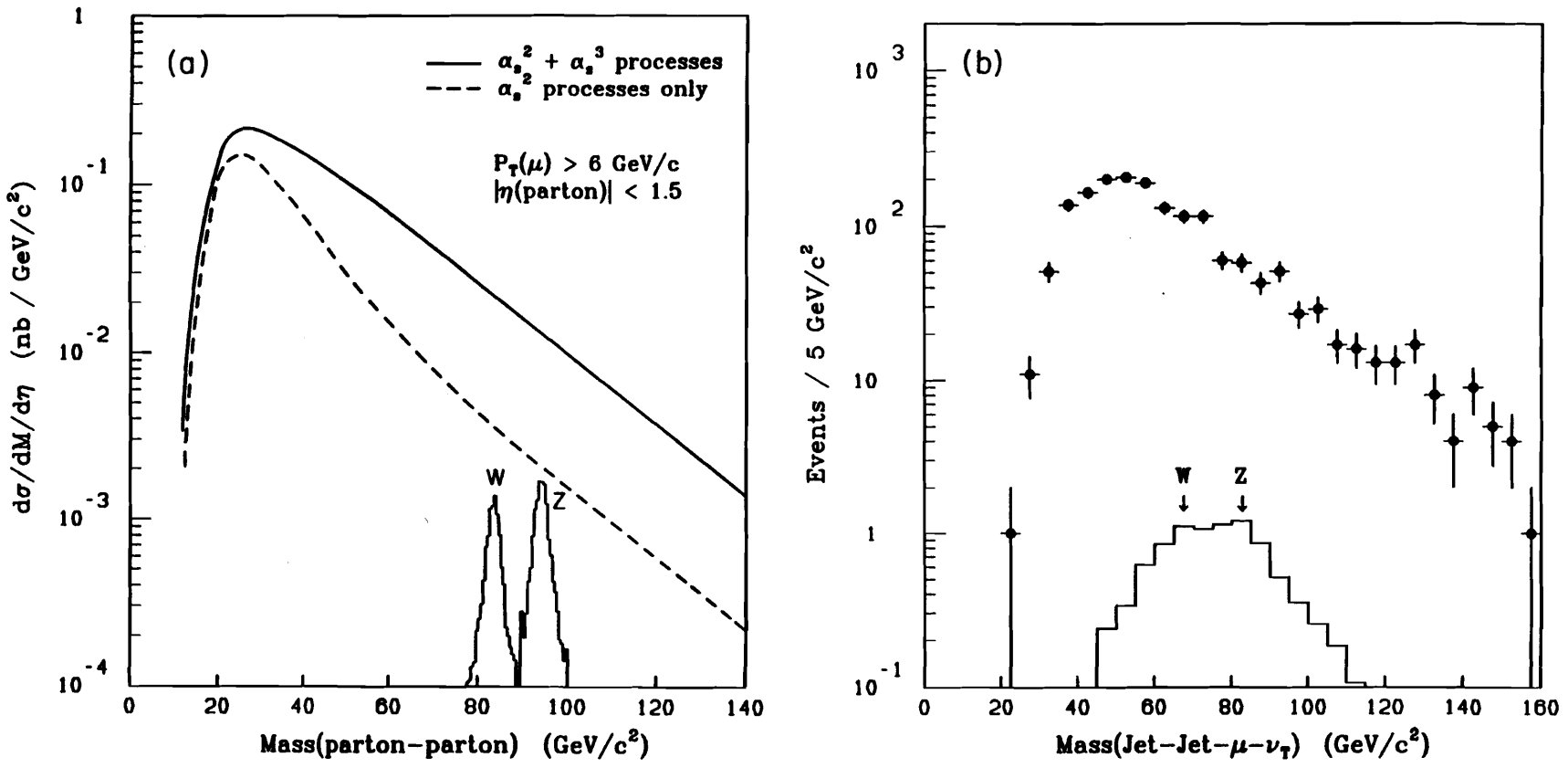

Fig. 5. a) Parton-parton invariant mass distribution calculated in ISAJET for $Q\bar{Q}$ pairs ($Q \equiv c/b$) from strong production and from W/Z decay [6].

b) Experimental distribution of M(jet-jet-μ-ν_T) for jet pairs with a muon of $p_T > 8$ GeV/c associated with one jet. The histogram shows a Monte Carlo calculation of the component due to W/Z decay [6].

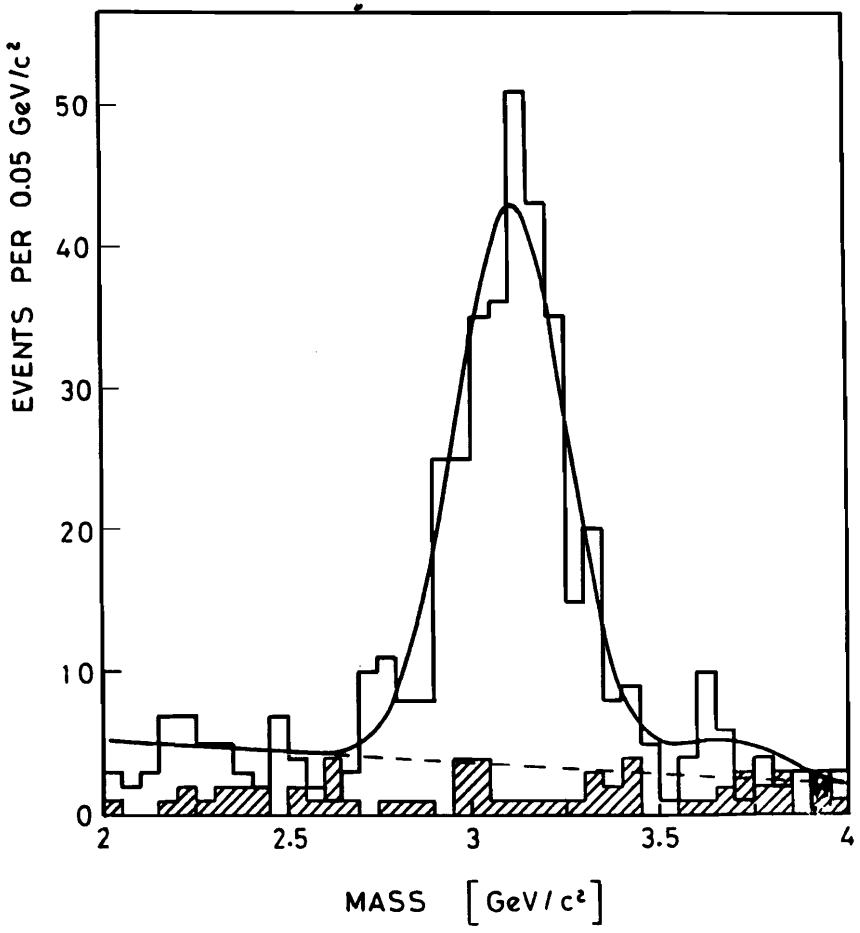

Fig. 6. Dimuon invariant mass for unlike-sign muon pairs. The fitted Gaussian has a mean value of 3.110±0.011 GeV/c^2 and a standard deviation of 0.15±0.01 GeV/c^2 [7].

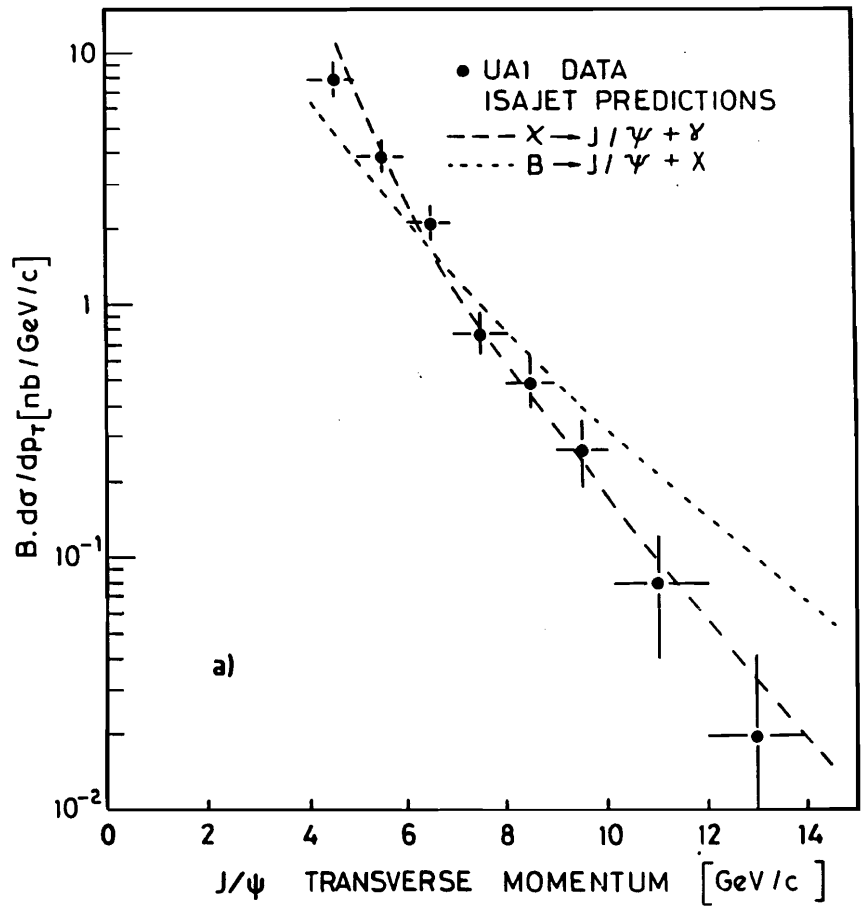

Fig. 7. The differential cross section, $B \cdot d\sigma/dp_T$, for $p\bar{p} \rightarrow J/\Psi + X$, $J/\Psi \rightarrow \mu^+\mu^-$ for $|y| < 2$. The Monte Carlo predictions are normalised to the data for $p_T > 5$ GeV/c [7].

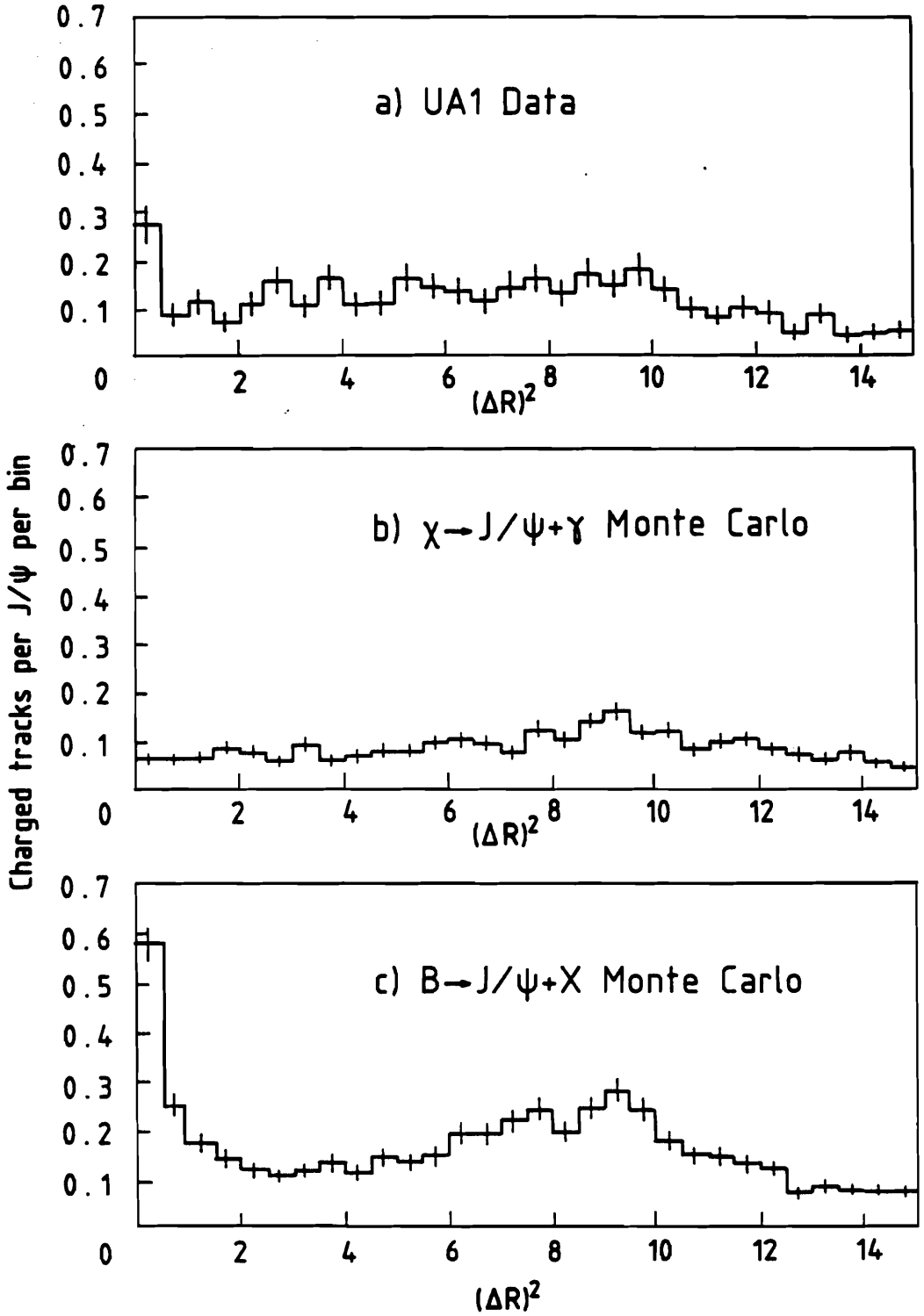

Fig. 8. Distribution in $(\Delta R)^2$ relative to the J/Ψ direction of charged tracks with $p_T > 1$ GeV/c for (a) data and (b,c) Monte Carlo calculations of J/Ψ production via decay of χ and B-hadrons respectively [7].

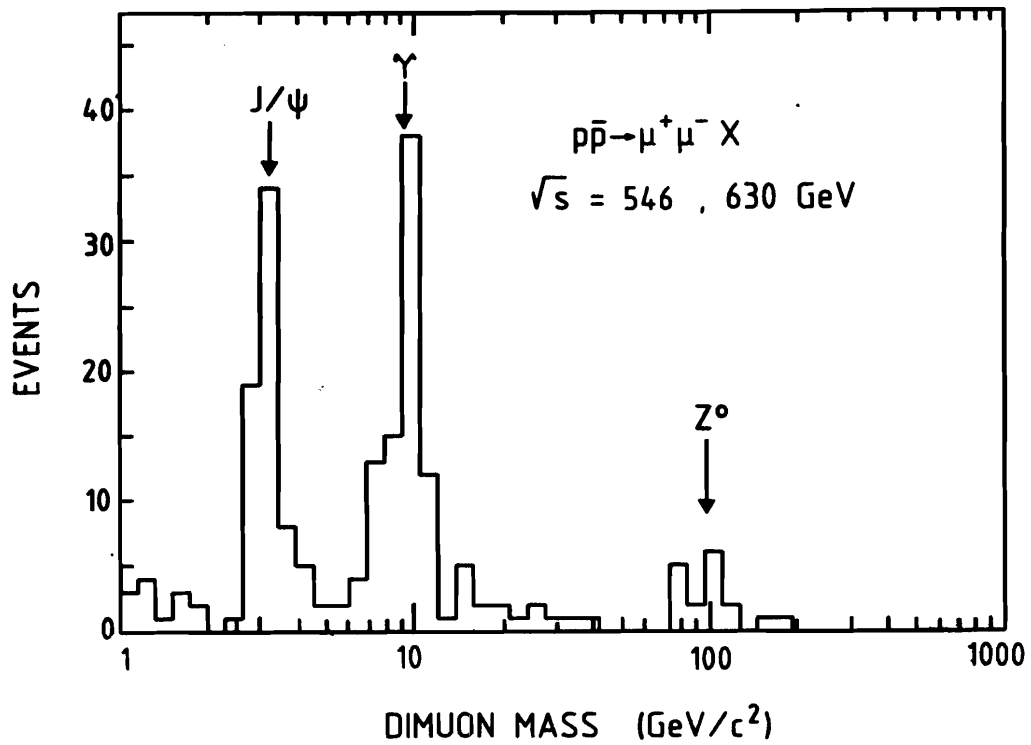

Fig. 9. Dimuon mass distributions for 235 isolated unlike sign dimuon events with $p_T(\mu) > 3$ GeV/c.

Table 3. Muon trigger rates at a luminosity of $L=5\times10^{30}$ cm^{-2}s^{-1} for different configurations of the UA1 detector [8].

Trigger Area	Trigger	Trigger Rate ($L=5\times10^{30}$ cm^{-2}s^{-1}) [Hz]		
		present configuration	with new calorimeter	and new shielding
90° ($\|\eta\| < 0.9$)	1μ	18	8	8
$0.9 < \|\eta\| < 1.7$	1μ	75	34	11
$1.7 < \|\eta\| < 2.1$	1μ	395	81	20

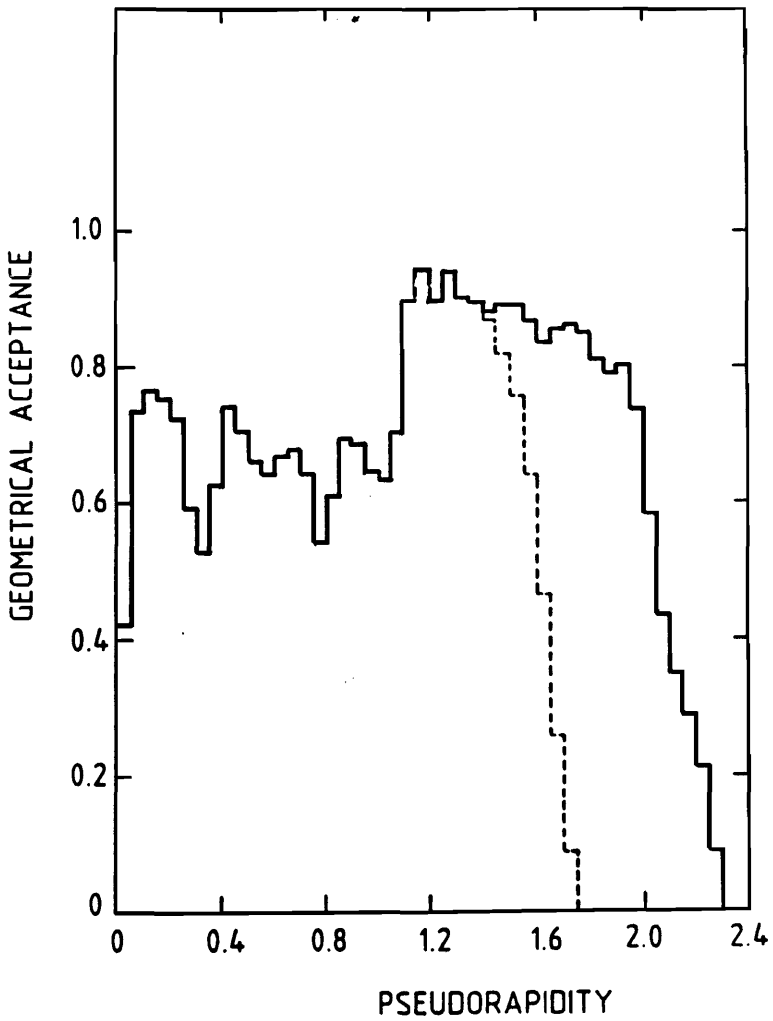

Fig. 10. Geometrical acceptance of the muon chambers. The broken line shows the triggering limit for inclusive single muons.

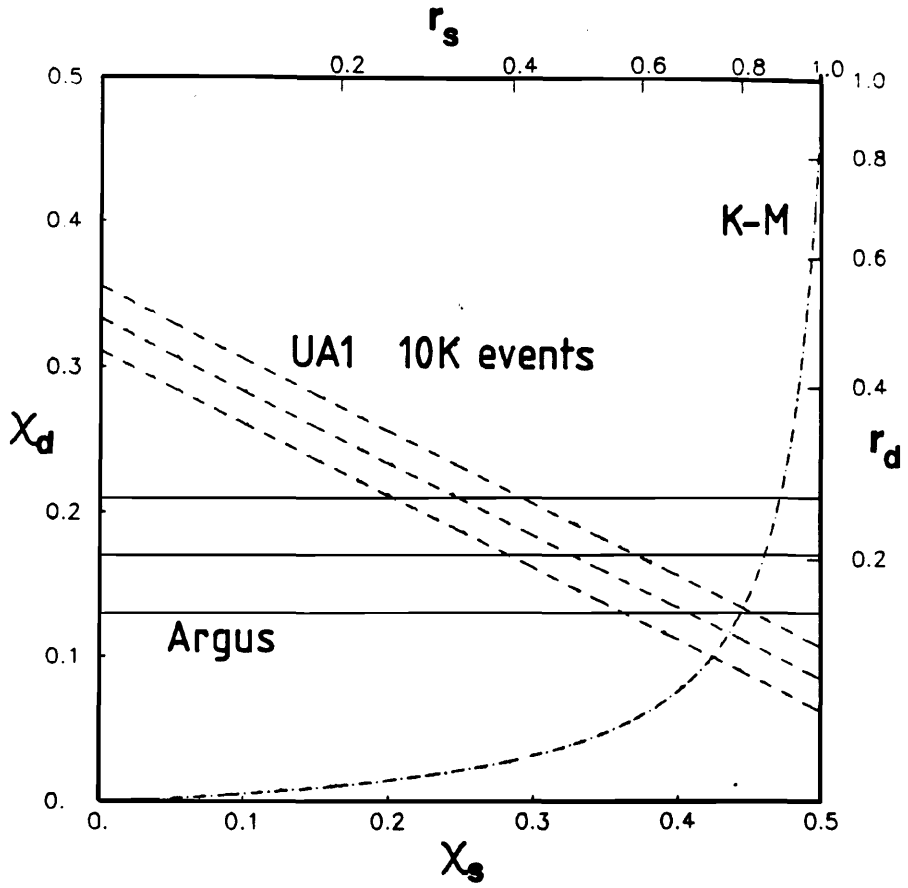

Fig. 11. Prospects for measuring the $B\bar{B}$ mixing parameters at ACOL. The current UA1 result [1] is shown along with the statistical error expected for 10^4 dimuon events.

parameters will constitute a strong test the Standard Model and is a major goal of the UA1 experiment.

A large dimuon sample could also be used to investigate heavy quark production mechanisms as illustrated in fig. 4 and discussed in Section 3.1.1. CP violation effects are probably out of reach, requiring a sample of $\approx 10^8$ dimuons.

So far the possibility of an electron trigger for $B\bar{B}$ events in UA1 has not been addressed. Electrons in the original UA1 detector, even when isolated, were increasingly contaminated by hadronic background ("pileup") below p_T of 15 GeV/c [9]. The fine-grained ($\Delta\theta \times \Delta\phi = 5° \times 6°$) uranium/tetramethyl pentane (TMP) calorimeter, currently under construction for the UA1 detector [10], will enhance the possibility of identifying electrons in the neighbourhood of jets. For example a recent study indicates that with the new calorimeter the second level trigger could find electrons ($p_T > 12$ GeV/c) inside b/c jets with 56% efficiency [11].

3. Comparative B-Physics Capability of Current Collider Detectors

The UA1, UA2, CDF and DØ detectors have the same basic structure [12]. The UA1 experience can therefore help us infer the potential for B-physics of the CDF and DØ experiments. From UA1 we learned that a high p_T muon trigger is effective in selecting $B\bar{B}$ production events. An integrated luminosity of 0.6 pb^{-1} gave a final physics sample of 20K single muon events with $p_T(\mu) > 6$ GeV/c and 500 dimuon events with $p_T(\mu) > 3$ GeV/c; the decay-in-flight background in these samples is 50% and 25% respectively. The 10K prompt muon events, together with the measured $B\bar{B}$ cross section of ≈ 2 μb [1], (corrected for K factors [2]), imply an efficiency in UA1 of ≈ 0.01 for triggering on and reconstructing an identifiable $B\bar{B}$ event.

Because the lepton from semi-leptonic B decay is not in general isolated, an electron trigger is not effective; the best evidence for this statement is the inability of UA2 to detect $B\bar{B}$ production [5].

Silicon vertex detectors could greatly enhance the efficiency of B-particle identification in current collider detectors. For definitive B-decay studies particle identification and precise momentum measurement are also essential. CDF and UA1 have limited hadron identification capability based on ionisation loss in the central tracking chamber.

3.1 Muon Capability

We focus here on the relative muon capabilities of the UA1, CDF and DØ detectors. Table 4 lists some of the parameters relevant to muon triggering and reconstruction. UA1 and DØ have essentially complete muon coverage to within 15° and 5° ($|\eta| = 2$ and 3) respectively of the beams; CDF has coverage from 90° to 45° and from 16° to 3°. In addition to this large gap, CDF is also

Table 4. Parameters of the muon detection system for the UA1, DØ, and CDF detectors.

	UA1 (upgraded)	DØ	CDF
Muon Acceptance	$\theta > 15°$	$\theta > 10°$ (5°)	$\theta > 45°$
			$3° < \theta < 16°$
	$\lvert\eta\rvert < 2$	$\lvert\eta\rvert < 3$	$\lvert\eta\rvert < 1$
			$2 < \lvert\eta\rvert < 4$
Absorber (λ)			
central	10	7 + 6 (T)	5
forward	16	9 + 9 (T)	8 + 10 (T)
p_T^{min} (GeV/c)			
central	3	4	2
forward	2	2	7
Decay Path (m)			
central	1.3	0.9	1.7
forward	3.2	1.8	7.0
Cal. Segmentation (central)			
$\Delta\eta \times \Delta\phi$	$0.1 \times 6°$	$0.1 \times 6°$	$0.1 \times 15°$

handicapped by a thin absorber and consequent punch-through in the central region [13], and by the long decay path in front of the forward muon detector.

UA1 and DØ have comparable muon capability and both are superior to CDF; DØ has larger geometric acceptance and is more compact that UA1. The fine-grained calorimetry of DØ and the upgraded UA1 detector may also allow detection of a subset of electronic decays of B (Section 2.2).

3.1.1 Predicted Muon Rates in DØ [14] Figure 12 shows the expected DØ muon trigger rate at $L = 10^{30}$ due to muons from C- and B- hadron decays. This plot was obtained using ISAJET convoluted with the DØ muon trigger efficiency. The same calculation gives the ratio b/(b + c), (fig. 13), and the fraction of decay-in-flight muons (fig. 14) as a function of muon p_T. For an integrated luminosity of 1 pb^{-1} the Monte Carlo predicts a total of 10^5 identified dimuon events from c/b- quark production; the requirement of $p_T > 2$ GeV/c for each muon would reduce

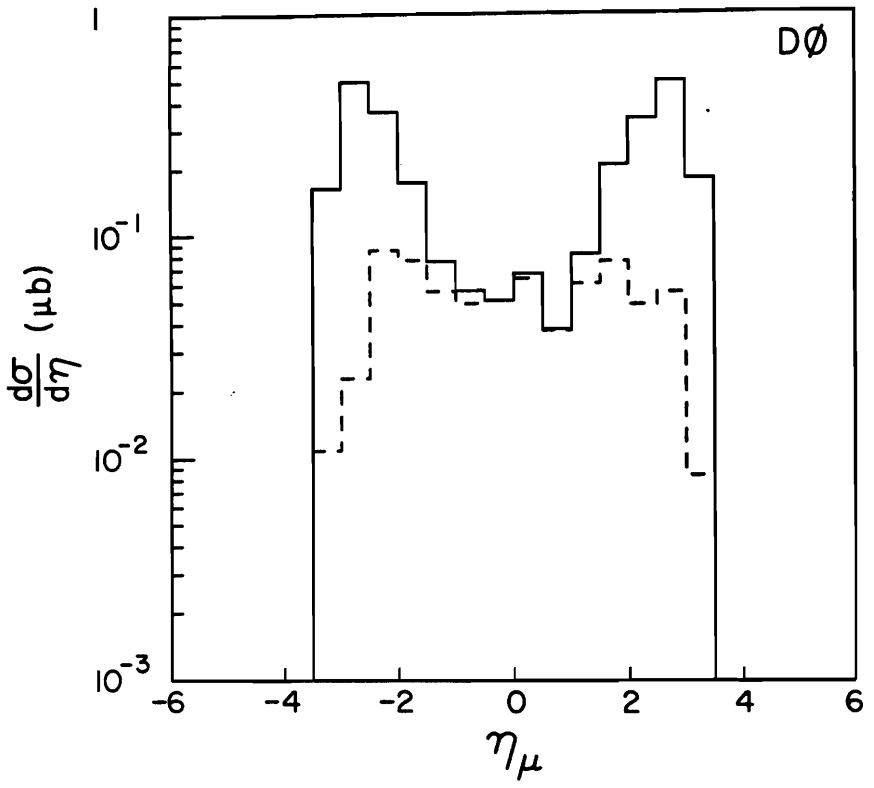

Fig. 12. Expected muon trigger rate in the DØ experiment versus pseudorapidity for luminosity of 10^{30} cm^2 s^{-1}; at this luminosity the trigger rate equals the cross-section in microbarns. The broken line corresponds to a minimum muon p_T of 4 GeV/c [14].

this number to 45K. It should be stressed that these numbers have not been corrected for muon reconstruction efficiency (≈ 33% in UA1)

The fraction of triggering muons which come from gluon splitting ($g \rightarrow b\bar{b}$) is predicted to increase steadily with muon p_T. Figure 15 shows the dimuon separation in ϕ and R, (η-ϕ space), expected for $b\bar{b}$ events with $20 < P_T(b) < 40$ GeV/c in the DØ detector. The gluon splitting component (dashed line) stands out.

3.2 Silicon Vertex Detectors

There is considerable interest in using silicon vertex detectors in collider detectors to tag secondary vertices from charm and beauty decays. The CDF group are close to testing a four-layer prototype detector [15]. UA1 has made detailed simulation studies [16] and a modest R & D effort is underway.

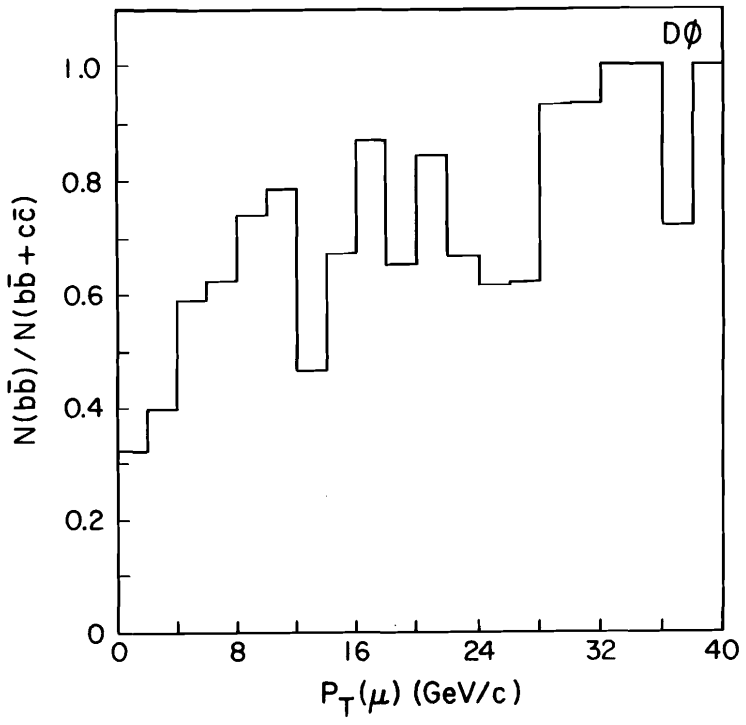

Fig. 13. ISAJET prediction for the ratio $N(b\bar{b})/N(b\bar{b} + c\bar{c})$ for events triggered by a muon in the DØ experiment [14].

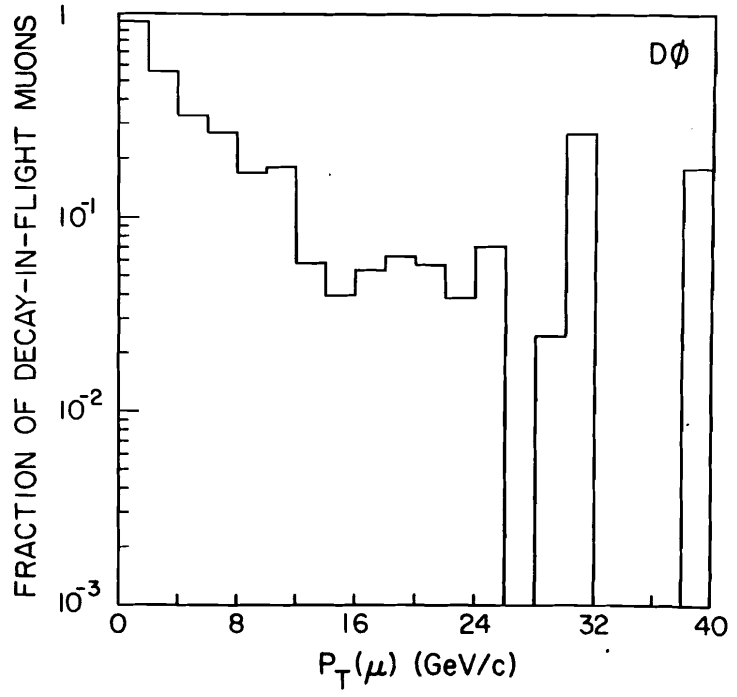

Fig. 14. Calculated fraction of π/K decay-in-flight muons as a function of muon p_T in the DØ experiment [14].

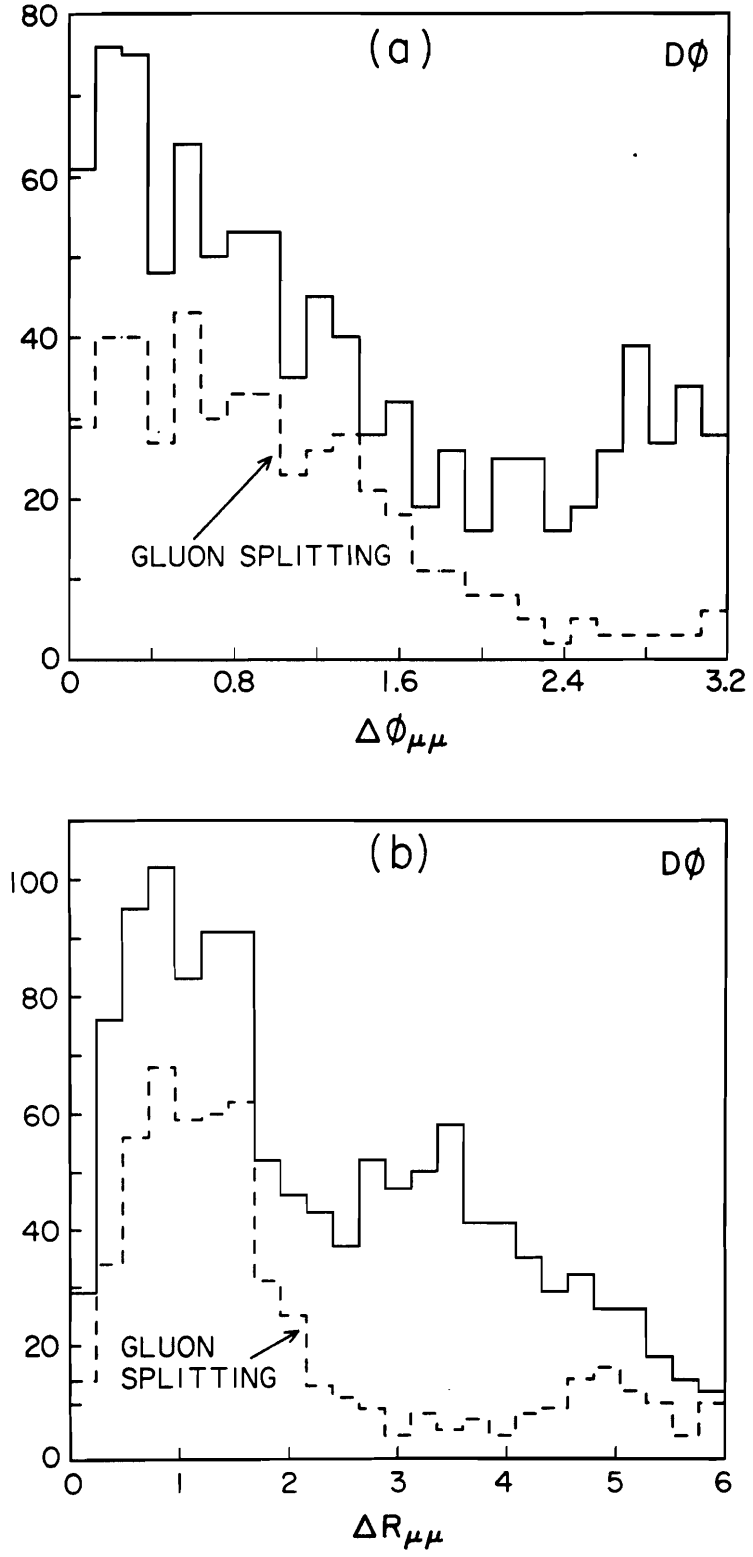

Fig. 15. ISAJET calculation of $\Delta\phi^{\mu\mu}$ and $\Delta R^{\mu\mu}$ for dimuons from $b\bar{b}$ events (p_T = 20-40 GeV/c) which pass the DØ muon trigger [14].

Figure 16 shows a schematic of the proposed CDF silicon vertex detector (SVX) and Table 5 lists some of the parameters. It consists of four layers of silicon surrounding the beampipe and centered at rapidity zero. The electrodes are parallel to the circulating beams. It will be read out by a low power CMOS Microplex chip currently under development at LBL. Figure 17 shows the expected resolution in impact parameter when the SVX is added to the CDF detector.

The horizontal dipole magnetic field of the UA1 detector dictates a "planar" geometry for a silicon vertex detector. One possible arrangement of four planes above and below the beampipe is shown in fig. 18; the electrodes are parallel to the magnetic field direction to optimize matching between track segments in the silicon detector and the central tracking chamber.

A detailed simulation using $B\bar{B}$ events generated by ISAJET with $8 < p_T < 16$ GeV/c has given the following results for the geometry shown in fig. 18 [15]:

i) the efficiency for tagging B-hadrons by impact parameter is about 10%,
ii) the efficiency for B-vertex reconstruction (with 3 or more tracks) is about 2%.

These relatively low efficiencies are due to the absence of coverage within ±45° in azimuth of the horizontal plane.

A simulation study of a silicon vertex detector in the DØ experiment is reported elsewhere in these proceedings [17]. The utility of this detector is limited by the absence of a central magnetic field in DØ.

Table 5. Parameters of the CDF silicon vertex detector.

Inner Radius	29 mm
Outer Radius	80.5 mm
Silicon Thickness	280 μ
Pitch	60μ (1,2,3), 110μ (4)
No. Channels	34,000
Readout	LBL CMOS μ-Plex Chip

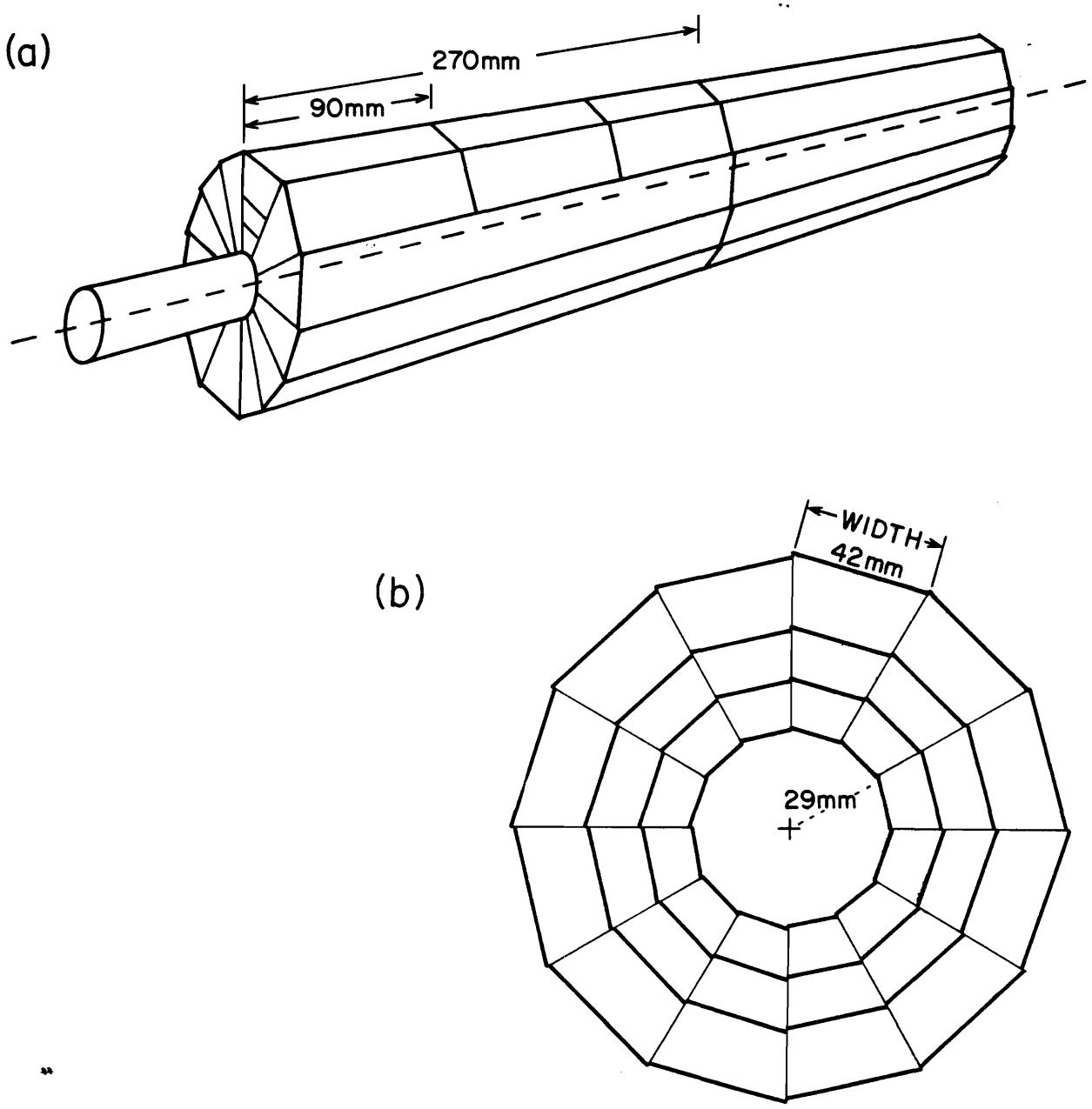

Fig. 16. Schematic of the CDF silicon vertex detector.

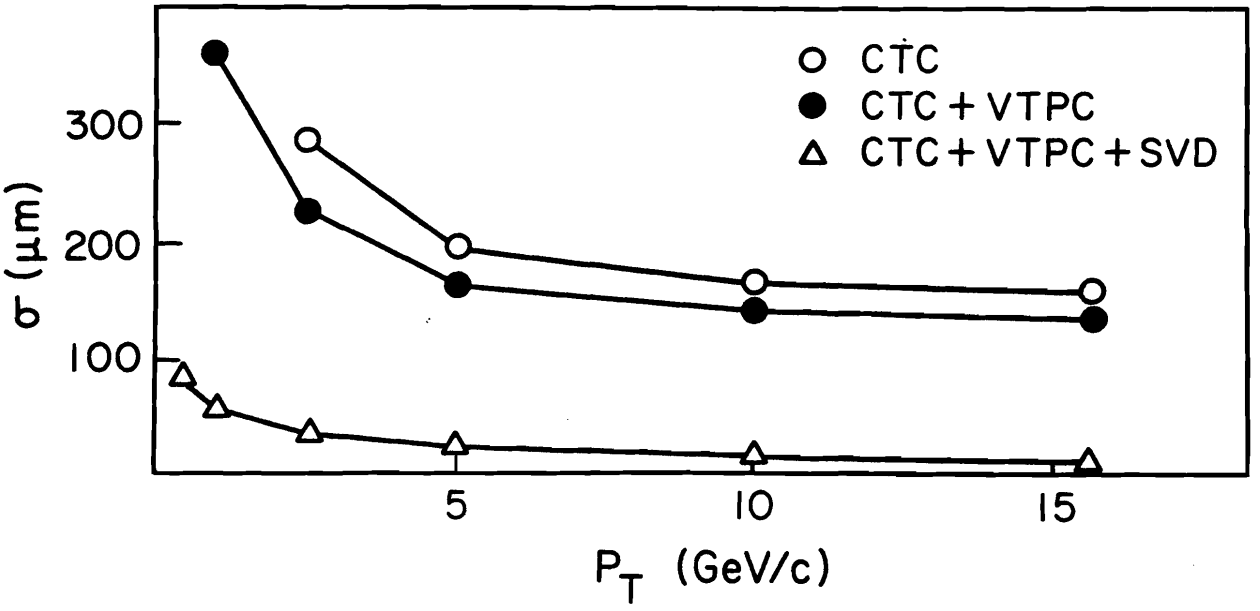

Fig. 17. Impact parameter resolution in the CDF detector before and after the addition of a silicon vertex detector.

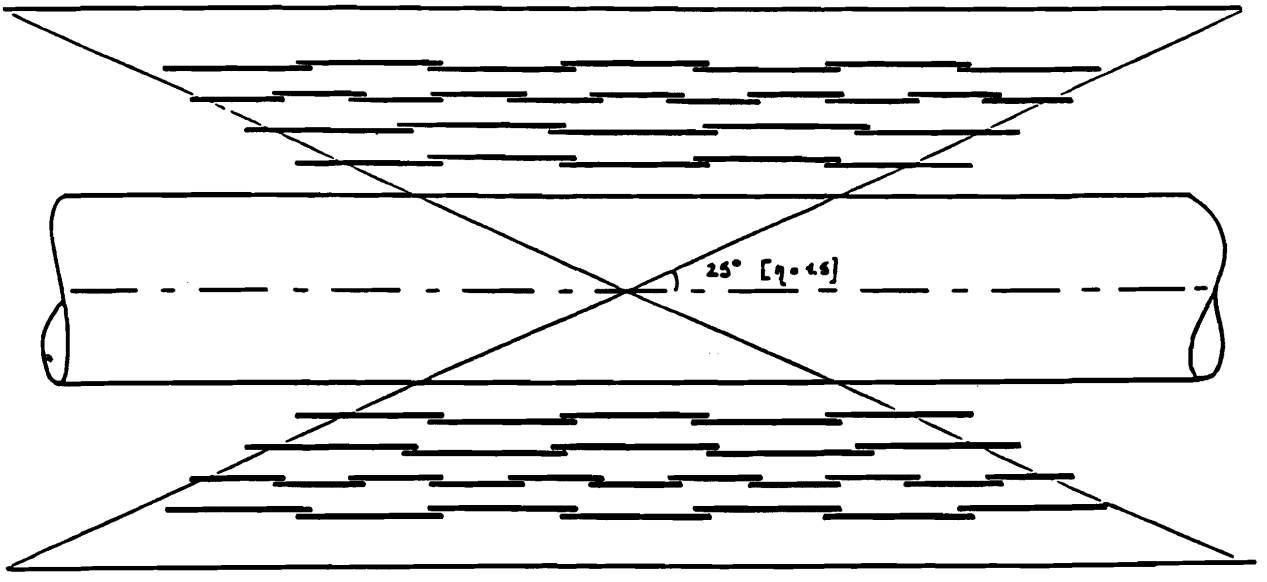

Fig. 18. A possible planar geometry silicon vertex detector for the UA1 experiment [ ].

4. CONCLUSIONS

The techniques available to the current collider detectors for $B\bar{B}$ detection are muon triggering and precision vertex detectors. The single muon trigger can provide an unbiassed sample of b-quarks for hadronization and decay studies. However experience indicates that this trigger is effectively limited to $p_T(\mu) \gtrsim 5$ GeV/c both by the need to control trigger rates and to avoid background from π/K decays in flight.

The Tevatron and CERN $p\bar{p}$ colliders producing about 10^6 (10^5) b–quarks per day at luminosities of $10^{30}cm^{-2}s^{-1}$ are indeed B–factories. However for the current collider detectors the effective luminosity is reduced at least two orders of magnitude by the inefficiency of the muon trigger.

The excellent muon capability of the UA1 and DØ detectors will permit significant studies of B^o–$\bar{B}^o$ mixing and heavy quark production mechanisms based on large samples (10^4–10^5) of dimuon events.

UA1 and CDF have good momentum resolution for charged particles. The addition of silicon vertex detectors to those experiments could allow the study of B lifetimes and decays. Both CDF and UA1, however, lack comprehensive particle identification; CDF is also limited by an inefficient muon system.

In summary the existing collider detectors are likely to play a major role in exploring the $B\bar{B}$ sector in the next few years. But many of the goals proposed in this workshop and others [18] are clearly out of reach. The achievement of these goals and the full exploitation of the b-quark flux at the Tevatron collider will require a detector specifically designed for this purpose.

---

1. C. Albajar et al., (UA1 Collaboration), Phys. Lett. 186B (1987) 237 and 247.

2. E.L. Berger, Argonne report ANL-HEP-CP-87-53 (June 1987), Proc. XXII Rencontre de Moriond, 1987, and "Benchmark Cross Sections for Bottom Quark Production", these proceedings.

3. F. Paige and S.D. Protopopescu, ISAJET Monte Carlo, BNL 38034 (1986).

4. C. Albajar et al., (UA1 Collaboration), "Study of Heavy Flavour Production in Events with a Muon accompanied by Jet (s) at the CERN Proton-Antiproton Collider, CERN-EP/87-189, Oct. 1987, submitted to Zeitschrift fur Physik.

5. L. Dilella, private communication.